Carrier Protein and Halogenase Selectivity in the Biosynthesis of Halogenated Pyrroles

Andrew J. Lail
Undergraduate Research Thesis
Georgia Institute of Technology
School of Chemistry and Biochemistry
Spring 2019

Principal Investigator: Dr. Vinayak Agarwal
Research Mentor: Dr. Hem Raj Thapa

Abstract

Natural product biosynthetic pathways often share similar architecture even when they lead to different final products. In polyketide synthase (PKS) and non-ribosomal peptide synthetase (NRPS) enzymatic pathways, the substrate is attached to a carrier protein (CP) while the tailoring enzymes make modifications to yield a final product. The CP may therefore have a role in determining what enzymes act on the substrate, influencing the final product's chemistry. In this study, pyrrole halogenases from several different bacterial species were characterized *in vitro* to test their ability to halogenate pyrrolyl CPs from four different natural product biosynthetic pathways. The reactions were analyzed via mass spectrometry to determine the halogenation state of the products formed. This study concludes that only some halogenases can act promiscuously on CPs from other pathways. Additionally, there is some modulation in the number of halogenation events between certain CP and halogenase pairs. The selectivity of these halogenase and CP interactions is likely caused by protein-protein interactions, and the structure of the CP/halogenase complex may provide new insights into such interaction.

Introduction

Natural products are small molecule metabolites from biological sources. They are found in all parts of the biosphere and have a diverse range of function in ecosystems. Organisms use these molecules for signaling, for chemical defense, and as allelochemicals (1-3). In addition to their functional diversity, their chemical diversity is pronounced. This has led to their use as drug candidates with action against tumors, inflammation, viruses, and bacteria (4, 5). Detailed understanding of natural product biosynthesis will allow us to more fully understand their natural role, as well as provide a platform for industrial production of complex chemical structures that are otherwise too expensive to be made from a chemical synthesis route (6).

There are some natural product pathways that share remarkably similar enzymatic machinery, including fatty acid synthesis (FAS), polyketide synthesis (PKS), and non-ribosomal peptide synthesis (NRPS). Each of these pathways takes small molecule building blocks and arranges them in modular structures to form highly complex final products. Through this strategy, organisms can take simple molecules like malonyl-CoA or amino acids and make specialized compounds for any number of purposes. The modular structure is facilitated by an assembly line layout of enzymes, with different enzymes carrying out specific modifications, then passing the growing product onwards. In most currently known pathways of this type, there is a CP that covalently binds the substrate while it is being modified by the other enzymes in the pathway. These CPs interact with the surfaces of other enzymes in a dynamic way, potentially helping to guide the substrate through the biosynthetic pathway (7).

Several similar natural product biosynthetic pathways that utilize the same general enzymology have been well characterized. For one specific motif, the halogenated pyrrole, there are at least four pathways leading to its production (Figure 1). The biosynthesis of pyoluteorin, an antifungal molecule with a chlorinated pyrrole, is encoded by the Plt gene cluster in *Pseudomonas fluorescence*, a soil bacterium (8). Similarly, the biosynthesis of chlorizidine A and its chlorinated pyrrole procedes by a polyketide synthase gene cluster (9). However, instead of being synthesized by a terrestrial microbe, this set of enzymes comes from the marine bacterium *Streptomyces* sp. CNH-287. Marinopyrrole is also from a marine bacterium (10). In addition to chlorinated pyrrole rings, brominated pyrrole products like tetrabromopyrrole are produced by the marine bacterium *Marinomonas mediterranae* MMB-1 (11). These examples, shown in Figure 1, show that enzymology for generation of a pyrrole scaffold is

widespread in bacteria from a variety of environments, which makes it a natural target for biochemical investigation.

The halogenated pyrrole biosynthesis starts with a free proline molecule (Figure 1). The proline is adenylated by the adenylation domain, using up ATP to attach an AMP moiety in place of the carboxyl group. Then, the adenylation domain attaches the proline to the pantetheine arm of the CP using AMP as the leaving group. This leaves a proline attached to the CP via a thioester bond. The proline is then dehydrogenated at two locations on the ring, generating the pyrrole. After that, the pyrrole ring is halogenated by the halogenase enzyme. The halogenated pyrrole ring is then further modified and incorporated into the final natural product structure, such as chlorizidine A or pyoluteorin.

Since these pathways are well characterized, they can be used to query the selectivity of CPs and halogenases. Using *in vitro* enzyme assays, this study combined CPs and halogenases across pathways in an attempt to generate halogenated pyrrole products. This experiment will inform on the selectivity of CPs towards their respective halogenases. Additionally, it will provide a new platform for developing cross-pathway natural products with novel chemistries, potentially harnessing pathways from diverse organisms to develop novel therapeutic molecules.

Methods and Materials

Protein Purification

Each of the proteins needed for the enzymatic assay was expressed recombinantly in *E. coli* using plasmids (Table 1). The halogenase enzymes Bmp2, Clz5, and Mpy16 were expressed to encode for His-MBP tag at their N-terminus using pET-28MBP vector. PltA halogenase was expressed to encode for His-tagged protein using the pET-28b vector. The CPs (Bmp1, PltL, Clz18, and Mpy15) were expressed with His tags using the pET-28b vector. PtdH, a phosphite dehydrogenase used to regenerate NADH cofactor was purified previously for other experiments, and it was used from a stock kept at -80°C.

Using *E. coli* cells transformed with the required plasmids, overnight cultures were grown at 37°C. One-liter cultures of TB liquid media were inoculated and allowed to reach 0.6 OD_{600} at 37°C. Recombinant protein expression was induced by 0.3 mM IPTG at 18°C for 18 hours with vigorous shaking. The culture was then centrifuged to collect the biomass in the pellet, which was resuspended in binding buffer (see Table 2 for all buffer compositions). The resuspended cells were sonicated for 15 minutes with stirring using a 10:50 on:off cycle, lysing the cells. After the cells were lysed, the solution was centrifuged at 13,500 rpm for 40 minutes to obtain supernatant. The supernatant was loaded onto a Nickel affinity chromatography column attached to an AKTA Prime FPLC system at 4°C and washed with 40 mL wash buffer. The protein was eluted with a 40 mL gradient of elution buffer ranging from 0% to 100%. Proteins were then dialyzed using dialysis buffer overnight. After dialysis, the protein solution was loaded onto an anion exchange column. The column was washed and the protein was eluted using IEX buffer B. Finally, the protein was put through a size exclusion PD-10 column for desalting and was eluted with storage buffer.

Synthesis of pyrrolyl-CP substrates

Proteins were stored at -80°C until they were ready to be used in an assay, at which point they were thawed on ice, vortexed gently, and centrifuged. Pyrrolyl-CP substrates were generated using purified CPs and organically synthesized pyrrolyl-pantetheine substrate. Multiple enzymatic transformations lead

to the pyrrolylpantetheine present in the biosynthetic pathway (shown in Figure 2). In this study, however, a pyrrole moiety was synthetically attached to a pantetheine molecule and this was enzymatically ligated to the CP using CoaA, CoaD, CoaE, and Sfp in a single pot reaction (Table 3) following the methods described previously (12). The Coa enzymes are naturally used in *E. coli* to prepare CP pantetheine groups, but they are promiscuous enough to accept a variety of altered pantetheine derivatives, including the pyrrolylpantetheine. The reaction products were purified on a Superdex 75 16/200 size exclusion chromatography column, equilibrated with 20 mM Tris-HCl (pH 8.0). The purified pyrrolyl-CP substrates were confirmed by LC-MS analysis.

Enzyme assays

The setup for enzyme assays is shown in Table 4. Assays were carried out in 100 µL reaction volumes held at 30°C for 3 hours. Each reaction contained 50 µM pyrrolyl-CP, 20 µM halogenase, 10 µM PtdH phosphite dehydrogenase, and 20 µM RebF flavin reductase, 20 mM HEPES buffer at pH 7.9, 200 mM KCl or KBr as a halide source, 1 mM NAD^+, 100 µM FAD, 10 mM sodium phosphite, 5 mM TCEP reducing agent, and final volume adjustment was done with 20% glycerol. Freshly prepared sodium phosphite was used in the reaction. After 3 hours, the reactions were quenched with a 1:1 mixture of acetonitrile and water. Once quenched, the reactions were centrifuged in a tabletop centrifuge at maximum speed for 30 minutes, and 20 µL of supernatant was analyzed by LC-MS.

Within the assay, the sodium phosphite provided the chemical energy for the product formation (Figure 4). The enzyme PTDH transforms phosphite into phosphate, making NADH in the process. This NADH is subsequently consumed by RebF, a flavin reductase, when it turns FAD+ into $FADH_2$. The $FADH_2$ powers the halogenase reaction. The entire enzymatic sequence is regenerated *in situ*, only consuming phosphite ion, which is provided in excess. The procedure is similar to previously described assays, differing mainly in source of flavin reductase (13).

Analysis of halogenated reaction products

Reaction products were analyzed on an Agilent 1260 infinity quaternary LC coupled to impact II ToF mass spectrometer. Data was acquired in the positive mode between 100 and 2000 m/z. All procedures were identical to those previously described (13). Data was analyzed by MS^1 (when available) and MS^2. The formula for deconvoluted mass = (ion mass x charge) – (mass of hydrogen x charge) was used to find the deconvoluted mass of the whole peptide in MS^1 (Figure 5A). For MS^2 analysis, the phosphopantetheine ejection ion was used to determine halogenated product. The phosphopantetheine with the pyrrolyl substrate attached gives an ejection ion at 354.15 m/z. From that mass, any addition of halogen attachments increases the ejection ion mass to charge ratio (Figure 3). For chlorine, mono-chlorination results in a 388.11 m/z ejection ion, while di-chlorination results in an ejection ion at 422.07 m/z. Additionally, the 422.07 m/z ion exhibits an isotopic envelope effect characteristic of chlorination (Figure 6). For bromination, the ejection ions have exact masses of 432.06 m/z (mono-bromination), 509.97 m/z (di-bromination), and 587.88 m/z (tri-bromination).

Results and Discussion

Synthesis of pyrrolyl-CP substrates

Products of the reaction to generate pyrrolyl-CPs were analyzed with LC-MS. If the pyrrolyl-CP substrate was successfully generated, an ejection ion at 354.15 m/z should be observed. In the absence of the

pyrrolyl-pantetheine ejection ion, the predominant MS^2 ion is the pantetheine ejection ion at 261.12 m/z corresponding to the holo-CP (Figure 2A). The holo-CP is a result of the *E. coli* phospantetheinyl transferase attaching a pantetheine moiety to the CP during recombinant protein expression. Only a small fraction of the recombinant CP is transformed into holo-CP. Detection of pantetheine ejection ions of 354.15 m/z and 261.12 m/z from the pyrrolyl-CP synthesis reaction shows successful generation of pyrrolyl-CP substrate (Figure 2B). Only one representative example for Bmp1 (CP) and pyrrolyl-Bmp1 (CP) is shown in Figure 2. Similar results hold true for pyrrolyl-PltL (CP), pyrrolyl-Clz18 (CP), and pyrrolyl-Mpy15 (CP).

Enzyme assay of CP with halogenase

Assay with Pyrrolyl-Bmp1 (CP) and halogenase

When assays were done to test the halogenase activity of Bmp2, PltA, and Mpy16 on pyrrolyl-Bmp1 (CP) substrate, none of the reactions showed evidence of halogenation, based on analysis of the MS^1 spectra and the MS^2 ejection ions (Figure 7). For the assay with Bmp2, the MS^1 analysis of the $[M+12H]^{+12}$ ion yielded a mass of 11,046 Da, which corresponds to the pyrrolyl-Bmp1 (CP) substrate. The MS^2 for the assay with Bmp2 also yielded exclusively ejection ion at 354 m/z, with no ejection ions of 432, 510, or 587 m/z, suggesting no halogenation reaction by Bmp2 (Figure 7A). The result is particularly concerning, as the Bmp1 and Bmp2 combination was meant to serve as a positive control. The reaction's failure is likely due to Bmp2 having degraded activity during storage. PltA combined with pyrrolyl-Bmp1 (CP) gave a $[M+12H]^{+12}$ ion with a monoisotopic mass of 921.5539, which corresponds to mass at 11,046 Da. This is the mass for the pyrrolyl-CP, the same as in the Bmp2 assay. When the MS^2 spectrum was examined, it also gave no evidence of chlorination as ejection ions for chlorinated pyrrole were not detected and only ejection ions at 354 m/z were observed (Figure 7B). For the assay done with Mpy16 halogenase, pyrrolyl-Bmp1 (CP) showed a similar result as the $[M+12H]^{+12}$ ion gave a mass of 11,046 Da, corresponding to the pyrrolyl substrate, with no MS^2 evidence for halogenation (Figure 7D). The only halogenase that halogenated the pyrrolyl-Bmp1 (CP) substrate was Clz5, which showed a MS^2 ejection ion for mono-chlorinated pyrrolyl-CP product (Figure 7C). However, the predominant MS^2 ejection ion corresponded to the 354 m/z substrate suggesting low turnover of substrate by Clz5.

Assay with Pyrrolyl-PltL (CP) and halogenase

When pyrrolyl-PltL (CP) was used as a substrate with the various halogenases, every halogenase except Bmp2 resulted in a di-chlorinated product (Figure 8). Bmp2 once again showed no evidence of halogenation, with the only MS^2 ejection ion 354 m/z (Figure 8A). The MS^1 spectrum yielded a deconvoluted mass of 12,547 Da using the $[M+15H]^{+15}$ ion, corresponding to the pyrrolyl-CP substrate. As expected, the assay with pyrrolyl-PltL (CP) substrate and PltA halogenase produced a di-chlorinated product shown by the MS^2 ejection ion at 422 m/z (Figure 8B). The MS^1 analysis was not possible due to very noisy data. The MS^2 analysis of reaction product of halogenase Clz5 also resulted in 422 m/z ejection ion, showing the di-chlorination of pyrrolyl-PltL (CP) by Clz5 (Figure 8C). Similar to data from the PltA reaction, the MS^1 data was too noisy to interpret. Finally, Mpy16 halogenase also showed di-chlorination of pyrrolyl-PltL (CP) as evidenced by the MS^2 data showing a strong ejection ion at 422 m/z (Figure 8D).

Assay with Pyrrolyl-Mpy15 (CP) and halogenase

For the assay with pyrrolyl-Mpy15 (CP) and halogenase, the activity varied among halogenases (Figure 9). Bmp2 showed no evidence of halogenation, similar to the previous reactions with other CPs. The MS^2 spectrum showed a strong peak at 354 m/z but no peak that corresponded to either mono- or di-bromination (Figure 9A). Furthermore, the MS^1 data showed a $[M+12H]^{+12}$ ion that gave a deconvoluted

mass of 10,681 Da, which corresponds to the pyrrolyl-Mpy15 (CP) substrate. The halogenase PltA mono- and di-chlorinated the pyrrolyl-Mpy15 (CP) substrate, as evidenced by the presence of 388 m/z and 422 m/z MS^2 peaks (Figure 9B). For the MS^1 data, the predominant $[M+11]^{+11}$ ion gave a deconvoluted mass of 10,749 Da, which is 68 Da higher than the pyrrolyl-Mpy15 (CP) observed in the Bmp2 assay. The shift in mass can be explained by the exchange of two hydrogen atoms for two chlorine atoms, which should result in a 67.9 Da shift. This result shows that the predominant reaction product of PltA is di-chlorinated pyrrolyl-Mpy15 (CP). For Clz5, chlorinated product formation was less pronounced but still present (Figure 9C). The MS^1 analysis of the predominant $[M+11H]^{+11}$ ion gave a deconvoluted mass of 10,681 Da, once again corresponding to the pyrrolyl-Mpy15 (CP) substrate. However, analysis of the MS^2 data shows ejection ions of 388 m/z and 354 m/z. This shows that Clz5 mono-chlorinates pyrrolyl-Mpy15 (CP), but no evidence of di-chlorination was found. Mpy16 assayed with its native CP, pyrrolyl-Mpy15, did chlorinate the substrate, showing evidence of both mono- and di-chlorination. MS^1 analysis of the most prominent peak (the $[M+11H]^{+11}$ ion) gave a deconvoluted mass of 10,715 Da, which is a 34 Da mass change indicative of mono-chlorination. Consistent with this, the highest intensity ion in the MS^2 data was the 388 m/z ion along with 422 m/z and 354 m/z, corresponding to di-chlorinated product and pyrrolyl substrates respectively (Figure 9D). This result shows that Mpy16 can both mono- and di-chlorinate its natural substrate.

Conclusion

The results of the enzyme assays clearly show that halogenases can recognize pyrrolyl-CPs from across pathways and halogenate when analyzed by *in vitro* assays. The assays that showed no evidence of halogenation were mostly those involving Bmp2 as a halogenase, which could be explained by the specific preparation of Bmp2 used having lost its activity. The other assays that did not give evidence for halogenation were PltA with pyrrolyl-Bmp1 (CP) and Mpy16 with pyrrolyl-Bmp1 (CP). These enzymes in reaction showed chlorination activity, suggesting the observed result is not due to degradation of their activity. The selectivity that these enzymes display on pyrrolyl-CP substrate could be explained by protein-protein interactions between substrate and halogenase pair. It is possible that the CP and the halogenase must be in close proximity for their activity. Thus, there are likely to be motifs on both surfaces that facilitate interaction. The selectivity observed could be due to difference in amino acid residues between CP and halogenase pairs from different pathways. If some of these residues are different from species to species, it could lead to the selectivity that was observed.

One way to understand the protein-protein interaction between the halogenase and CP pairs is to crystallize them in complex and study the structure-function relationship between the two proteins. A similar strategy has recently been employed to determine the complex of a CP and an oxidase enzyme in the tetrabromopyrrole biosynthetic pathway (14). Such a crystal structure would provide a framework for visualizing the differences in amino acid sequence for each CP. In follow up to that, site mutagenesis experiments could be performed to validate information obtained from the structure of the CP and halogenase pairs complex.

This study of CP and halogenase selectivity has potential impacts in the pharmaceutical biosynthesis of halogenated molecules. Oftentimes, pharmaceuticals of interest have complicated chemical syntheses that can make it desirable to pursue a biosynthetic approach. By determining the selectivity of these CPs to related halogenase enzymes, we will be able to mix and match CP and halogenase pairs across pathways to obtain a designer natural product. Additionally, the results show that CPs and halogenases work together across a broad variety of bacterial sources.

Figures and Tables

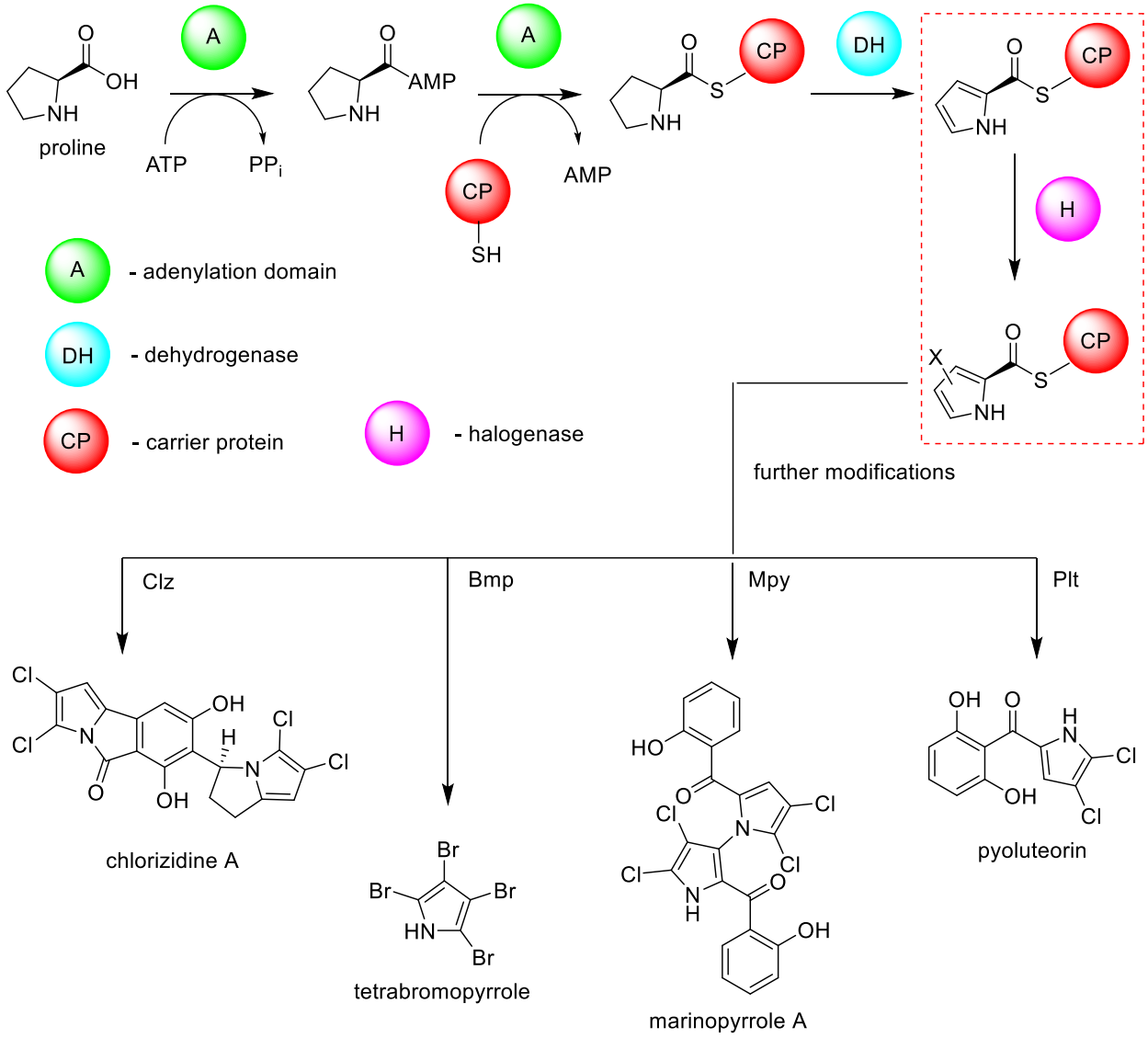

Figure 1: Generalized biosynthetic pathway for halogenated pyrrole biosynthesis, with final products chlorizidine A, tetrabromopyrrole, marinopyrrole A, and pyoluteorin shown. The proline starting molecule is attached to the carrier protein using ATP and an adenylation domain. Once attached, the proline is dehydrogenated, then halogenated by the halogenase. The reaction highlighted with the red box is the main reaction that this study focuses on, involving the carrier protein with the halogenase. Once halogenated, the pathways diverge and utilize unique enzymes to form the final products shown at the bottom of the figure.

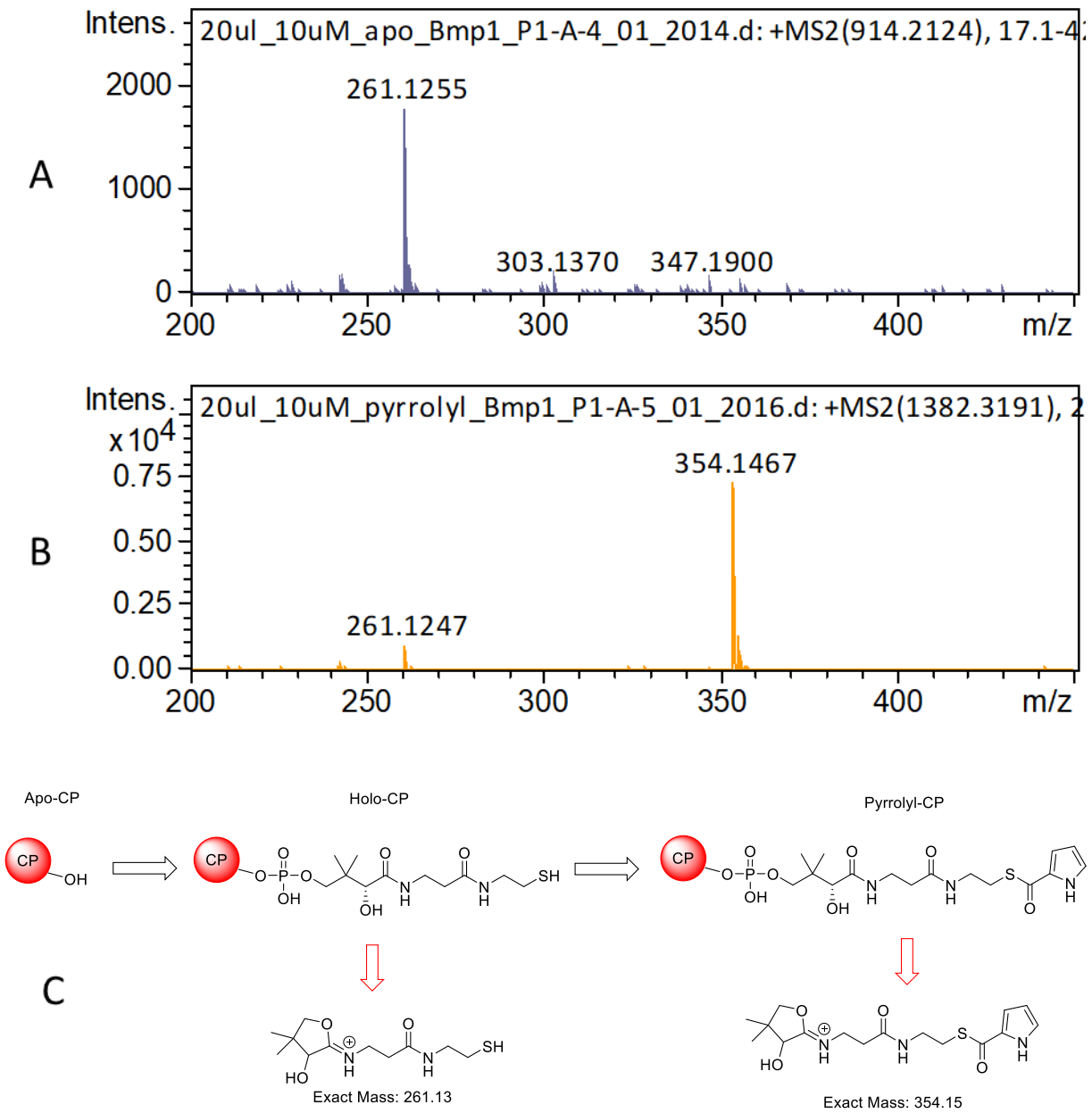

Figure 2: Comparison of MS^2 spectrum of Bmp1 (CP) and pyrrolyl-Bmp1 (CP). The 354.15 m/z ejection ion indicates the presence of the pyrrolyl-pantetheine group. Panel A shows the MS^2 ejection ion at 261.12 m/z of holo-CP protein. The holo-CP is evident at 261.12 m/z, while the apo-CP has no MS^2 ejection ion. Panel B shows the MS^2 spectrum of the pyrrolyl-CP, with the characteristic ejection ion at 354.15 m/z and 261.12 m/z in the CP protein generated from pyrrolyl-CP synthesis reaction. Since the holo-CP cannot react in the substrate synthesis reaction in this study, the 261.12 m/z peak is present in the pyrrolyl-CP spectrum as well. Panel C shows the structures of the apo-, holo-, and pyrrolyl-CPs and their associated ejection ions.

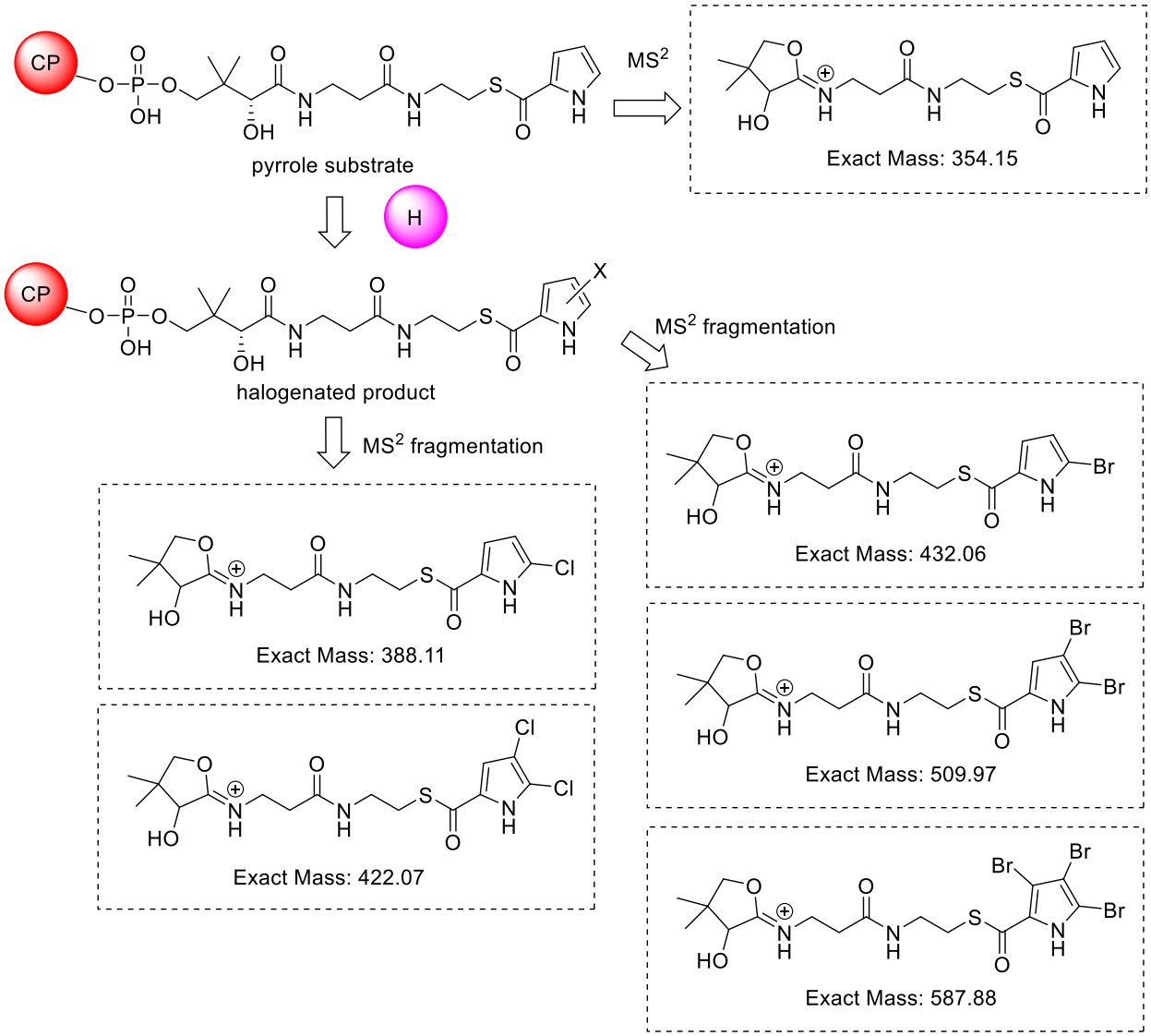

Figure 3: The enzymatic logic of product formation, along with the ejection ions indicative of each halogenation state. The pyrrolyl substrate was attached to the CP chemically. Reactions were monitored by looking for MS^2 ion fragments corresponding to each halogenation state. The 354.15 m/z ion shows that halogenation has not taken place, while the chlorinated and brominated MS^2 fragments each show characteristic mass to charge ratios.

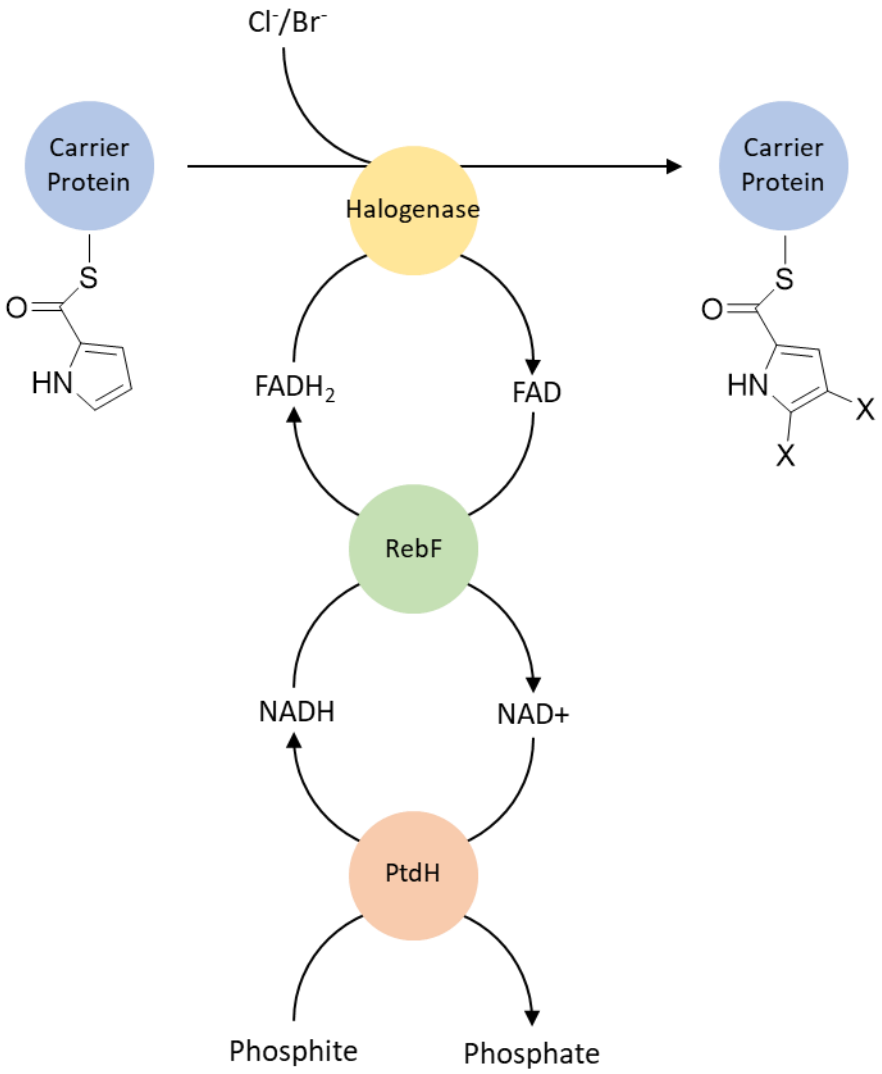

Figure 4: Reaction scheme for enzymatic assays. The pyrrolyl CP was acted on by the halogenase, which requires $FADH_2$ as a cofactor, as well as a source of halide ion. The $FADH_2$ is regenerated *in situ* by flavin reductase RebF, which itself is powered by NADH. NADH is regenerated from NAD^+ by the phosphite dehydrogenase enzyme PtdH. PtdH is powered by an excess of phosphite ion.

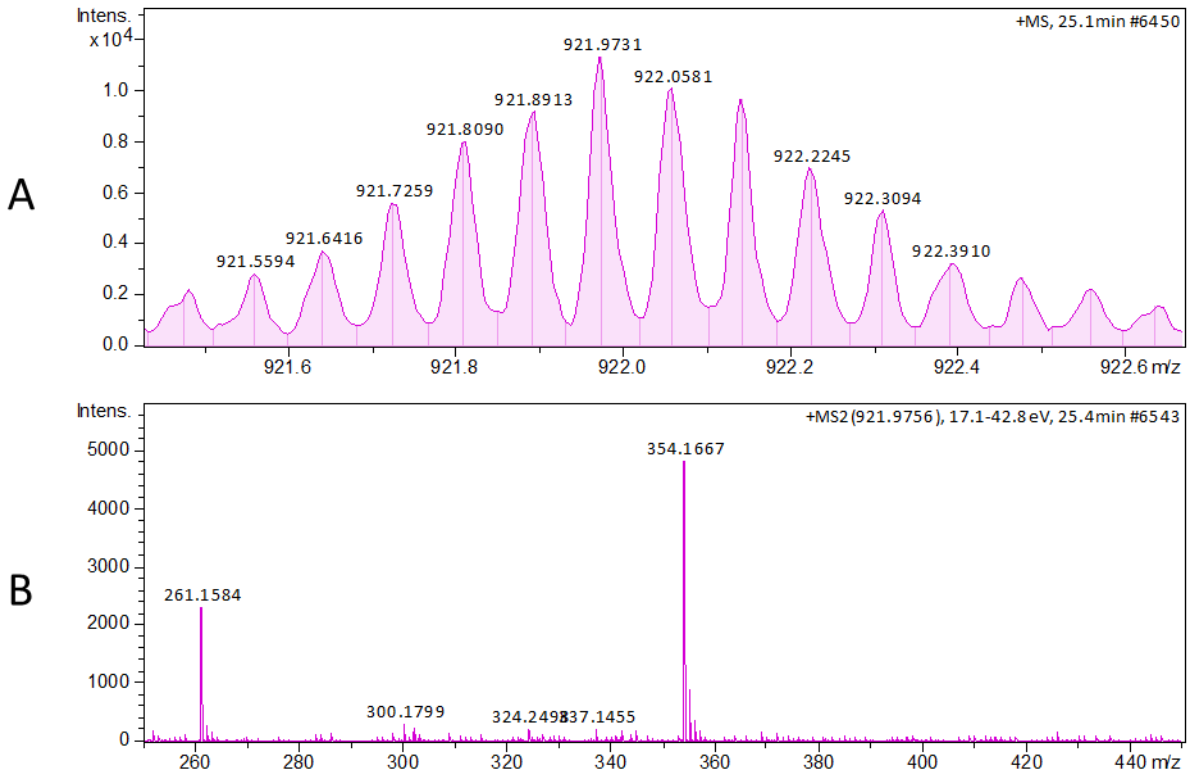

Figure 5: Representative MS spectra used for analyzing halogenation state. Shown here is the reaction product from the assay done with pyrrolyl-Bmp1 (CP) and Bmp2 halogenase. **A)** The MS^1 data shows a peak at 921.9731 m/z that corresponds to a $[M+12H]^{+12}$ ion. Using the formula mass = (monoisotopic mass x z) – (z x mass of H^+), the mass of the CP was determined to be 11,046.59 Da, which is the mass of the pyrrolyl-Bmp1 (CP) substrate. **B)** The MS^2 spectrum from the pyrrolyl-Bmp1 (CP) parent ion shows that the phosphopantetheine arm is not halogenated. Its 354 m/z corresponds to the pyrrole substrate, while the 261 m/z ion results from breakdown of the 354 m/z ion.

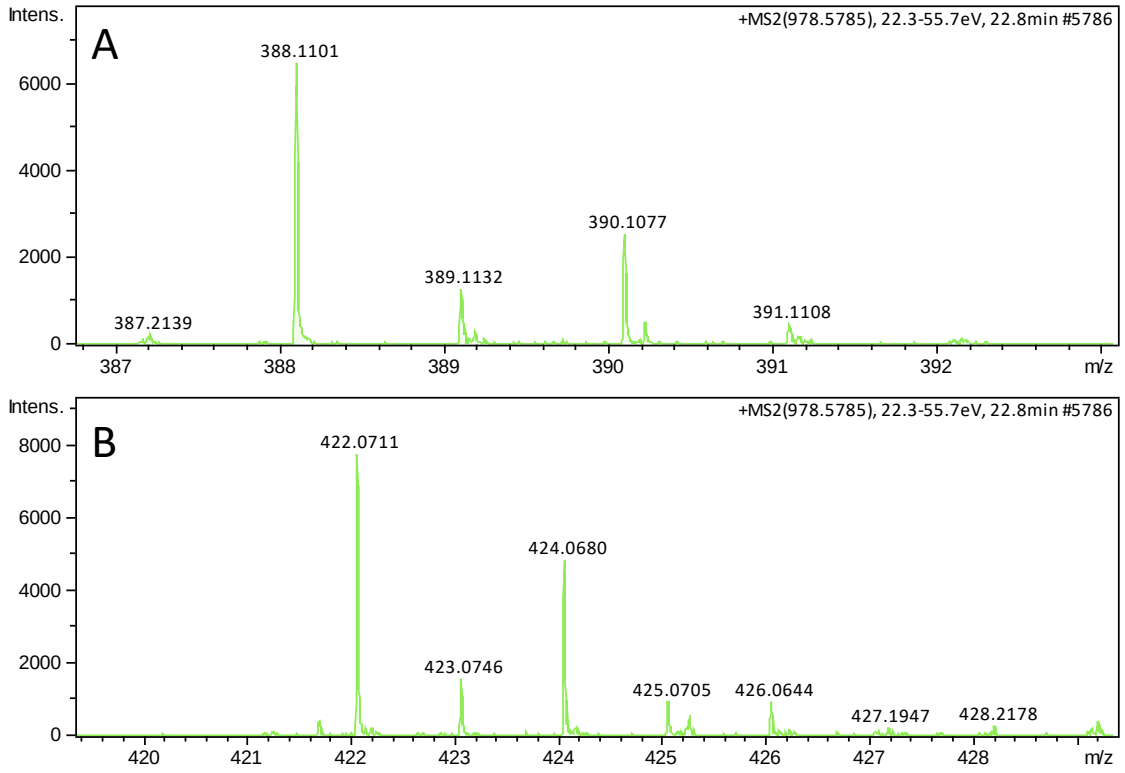

Figure 6: Representative MS^2 ion showing isotopic signatures of mono- and di-chlorinated species from the reaction of pyrrolyl-Mpy15 (CP) with PltA halogenase. The 388 m/z ion **(A)** corresponds to the monochlorinated pyrrole ring, while the 422 m/z ion **(B)** corresponds to the di-chlorinated species.

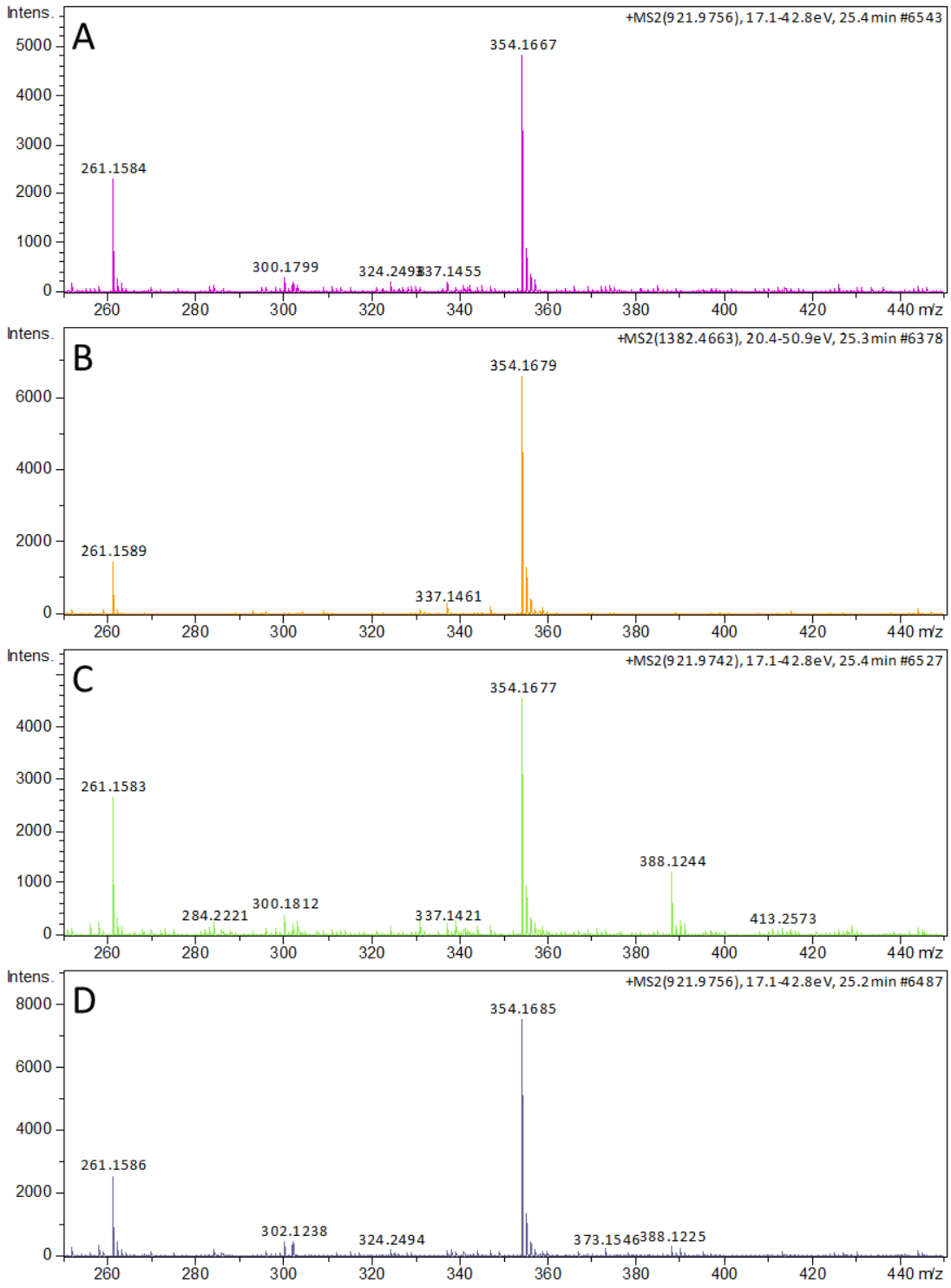

Figure 7: MS^2 spectra from the reaction of pyrrolyl-Bmp1 (CP) with different halogenases. The MS^2 data for each enzymatic reaction clearly shows the halogenation state of the products. Bmp2 (**A**), PltA (**B**), and Mpy16 (**D**) have peaks at 261 m/z (native phosphopantetheine ejection ion) and at 354 m/z (pyrrolyl substrate). Only Clz5 (**C**) shows any evidence of 388 m/z ejection ion, which corresponds to the monochlorinated product.

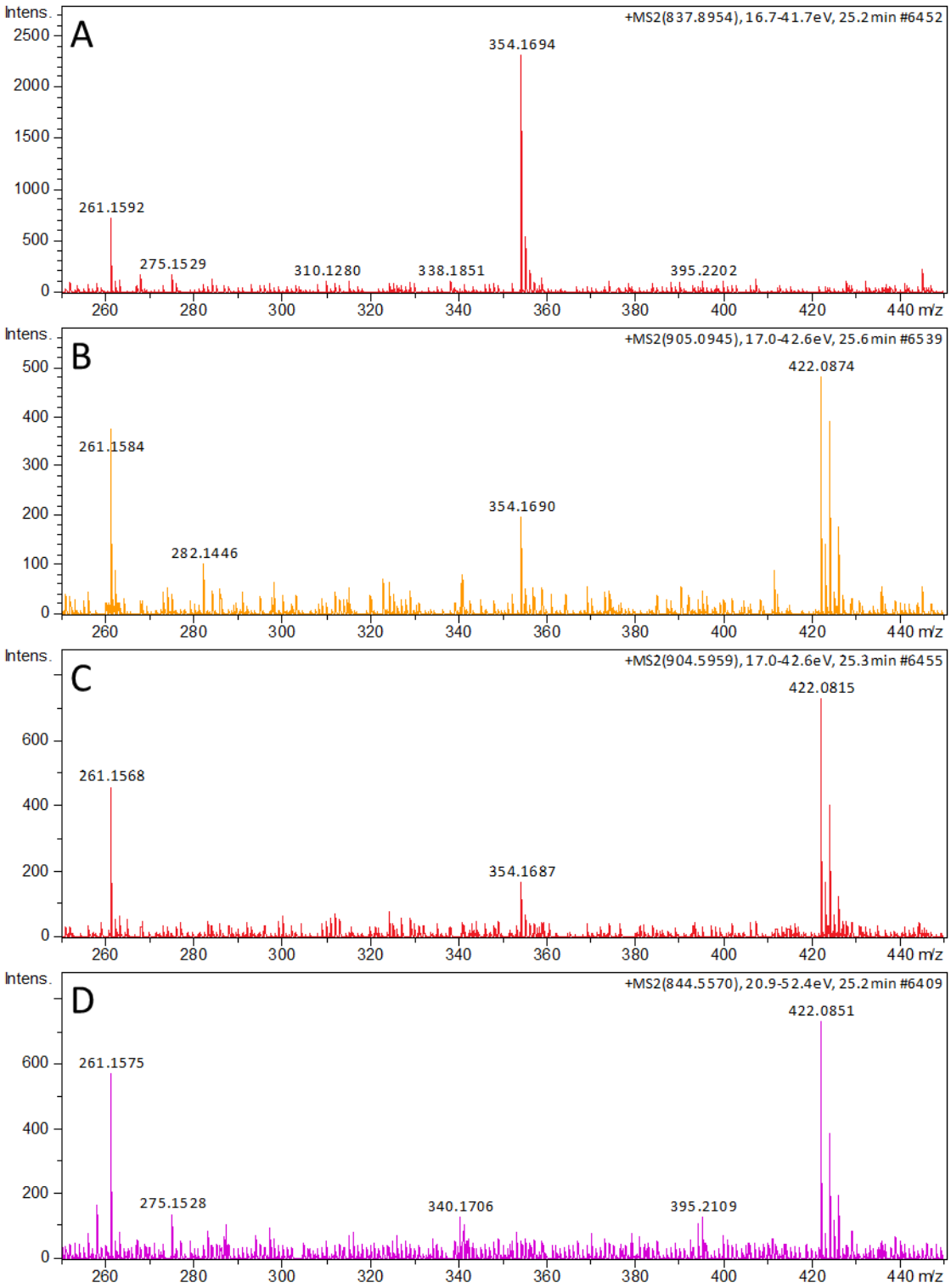

Figure 8: MS^2 spectra from the reaction of pyrrolyl-PltL (CP) with different halogenases. Bmp2 (**A**) showed no evidence of halogenation. Each of PltA, Clz5, and Mpy16 (**B-D**, respectively) di-chlorinated exclusively, with no mono-chlorinated intermediates observed.

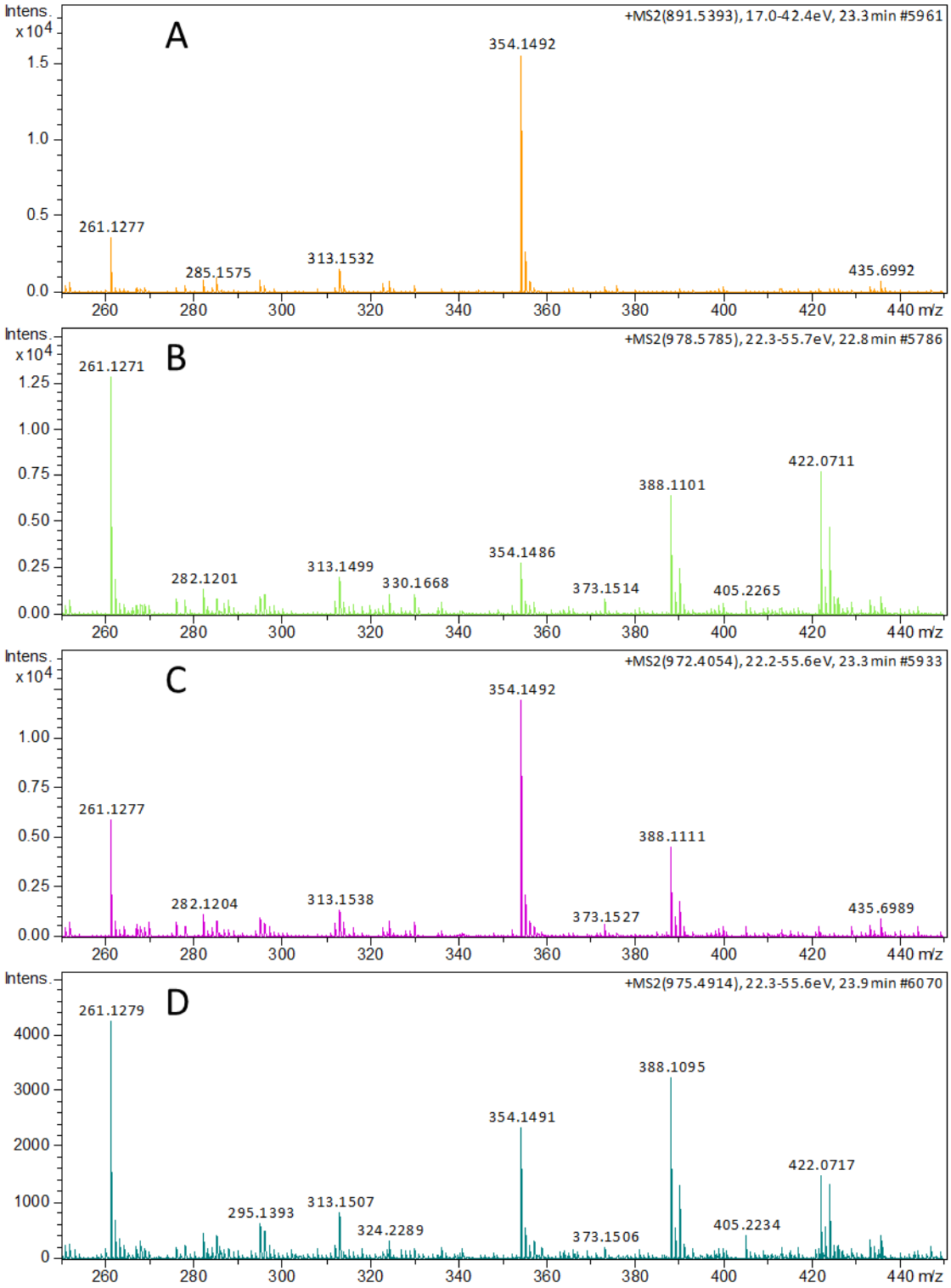

Figure 9: MS^2 spectra from the reaction of pyrrolyl-Mpy15 (CP) with different halogenases. Bmp2 (**A**) showed no evidence of halogenation, while Clz5 produced a mono-chlorinated product (**C**). PltA (**B**) and Mpy16 (**D**) both led to formation of mono- and di-chlorinated products.

Table 1: Constructs used to express proteins used in this study. Each protein was expressed in *E. coli* BL21 cells.

Construct	Fusion Tag	Plasmid Backbone	Source Organism	Reference
Bmp1	N-terminal His_6	pET-28b(+)	*M. mediterranea* MMB-1	(11)
Bmp2	N-terminal His_6	pET-28b(+)	*M. mediterranea* MMB-1	(11)
PltL	N-terminal His_6	pET-28b(+)	*P. fluorescens* Pf-5	(8)
PltA	N-terminal His_6	pET-28b(+)	*P. fluorescens* Pf-5	(8)
Clz18	N-terminal His_6	pET-28b(+)	*Streptomyces* sp. CNH-287	(9)
Clz5	N-terminal His_6 with Maltose Binding Protein	pET-28b(+)	*Streptomyces* sp. CNH-287	(9)
Mpy15	N-terminal His_6	pET-28b(+)	*Streptomyces* sp. CNQ-418	(10)
Mpy16	N-terminal His_6 with MBP	pET-28b(+)	*Streptomyces* sp. CNQ-418	(10)
PtdH	N-terminal His_6	pET-15b(+)	*Pseudomonas stutzeri*	(15)
RebF	N-terminal His_6	pET-28b(+)	*Lechevalieria aerocolonigenes*	(16)

Table 2: Buffer composition for protein purification.

Buffer Name	Composition
Binding Buffer	20 mM Tris 500 mM NaCl 10% Glycerol pH 8
Wash Buffer	20 mM Tris 30 mM Imidazole 1 M NaCl pH 8
Elution Buffer	20 mM Tris 250 mM Imidazole 1 M NaCl pH 8
Dialysis Buffer	20 mM Tris 50 mM KCl pH 8.9
IEX Buffer A	20 mM Tris pH 8.9
IEX Buffer B	20 mM Tris 1 M KCl pH 8.9
Storage Buffer	20 mM HEPES 50 mM KCl 10% glycerol pH 7.5

Table 3: Reaction setup for synthesis of pyrrolyl-CPs. The pyrrolyl-pantetheine substrate is modified *in situ* by CoaA, CoaD, and CoaE to yield an acyl-CoA molecule. This acyl-CoA is then transferred to the CP by Sfp to form a pyrrolyl-CP.

Component	Final Concentration	Function in assay
HEPES pH 7.9	50 mM	Buffer
$MgCl_2$	10 mM	Cofactor
Pyrrolyl-pantetheine	1 mM	Reactant
CoaA	1 µM	Pantothenate kinase
CoaD	1 µM	Phosphopantetheine adenylyltransferase
CoaE	1 µM	Dephospho-CoA kinase
Sfp	2 µM	Phosphopantetheinyl transferase
Purified CP	250 µM	Substrate
ATP	9 mM	Chemical energy
dH_2O		Volume adjustment

Table 4: Components of each enzymatic assay. The component, its function, and the final concentration is given. Each reaction had a total volume of 100 µL, adjusted to that exact volume with 25-60 µL of 20% glycerol.

Component	Final Concentration	Function in Assay
HEPES (pH 7.9)	20 mM	Buffer
KCl or KBr	200 mM	Halide Source
NAD^+	1 mM	Cofactor
FAD	100 µM	Cofactor
NaPhosphite	10 mM	Chemical energy
TCEP	5 mM	Buffer
Pyrrolyl-CP	50 µM	Substrate
Halogenase	20 µM	Enzyme
PTDH	10 µM	Cofactor regeneration
RebF	20 µM	Cofactor regeneration
20% Glycerol		Volume adjustment
	total 100 µL	

References

1. Pawlik JR (1993) Marine invertebrate chemical defenses. *Chemical Reviews* 93(5):1911-1922.
2. Li K*, et al.* (2018) Fatty-acid derivative acts as a sea lamprey migratory pheromone. *Proceedings of the National Academy of Science USA* 115(34):8603-8608.
3. Rasher DB, Stout EP, Engel S, Kubanek J, & Hay ME (2011) Macroalgal terpenes function as allelopathic agents against reef corals. *Proceedings of the National Academy of Science USA* 108(43):17726-17731.
4. Villa FA & Gerwick L (2010) Marine natural product drug discovery: Leads for treatment of inflammation, cancer, infections, and neurological disorders AU - Villa, Francisco A. *Immunopharmacology and Immunotoxicology* 32(2):228-237.
5. Newman DJ & Cragg GM (2016) Natural Products as Sources of New Drugs from 1981 to 2014. *Journal of Natural Products* 79(3):629-661.
6. Shen B (2004) Accessing Natural Products by Combinatorial Biosynthesis. *Science Signaling* 2004(225):pe14.
7. Drake EJ*, et al.* (2016) Structures of two distinct conformations of holo-non-ribosomal peptide synthetases. *Nature* 529:235.
8. Nowak-Thompson B, Chaney N, Wing JS, Gould SJ, & Loper JE (1999) Characterization of the Pyoluteorin Biosynthetic Gene Cluster of Pseudomonas fluorescens Pf-5. *Journal of Bacteriology* 181:2166-2174.
9. Mantovani SM & Moore BS (2013) Flavin-Linked Oxidase Catalyzes Pyrrolizine Formation of Dichloropyrrole-Containing Polyketide Extender Unit in Chlorizidine A. *Journal of the American Chemical Society* 135(48):18032-18035.
10. Yamanaka K, Ryan KS, Gulder TA, Hughes CC, & Moore BS (2012) Flavoenzyme-catalyzed atropo-selective N,C-bipyrrole homocoupling in marinopyrrole biosynthesis. *Journal of the American Chemical Society* 134(30):12434-12437.
11. Agarwal V*, et al.* (2014) Biosynthesis of polybrominated aromatic organic compounds by marine bacteria. *Nature Chemical Biology* 10(8):640-647.
12. Agarwal V*, et al.* (2015) Chemoenzymatic Synthesis of Acyl Coenzyme A Substrates Enables in Situ Labeling of Small Molecules and Proteins. *Organic Letters* 17(18):4452-4455.
13. Thapa HR, Lail AJ, Garg N, & Agarwal V (2018) Chemoenzymatic Synthesis of Starting Materials and Characterization of Halogenases Requiring Acyl Carrier Protein-Tethered Substrates. *Methods in Enzymology* 604:333-366.
14. Thapa HR, Robbins JM, Moore BS, & Agarwal V (2019) Insights into Thiotemplated Pyrrole Biosynthesis Gained from the Crystal Structure of Flavin-Dependent Oxidase in Complex with Carrier Protein. *Biochemistry*.
15. Johannes TW, Woodyer RD, & Zhao H (2007) Efficient regeneration of NADPH using an engineered phosphite dehydrogenase. *Biotechnology and Bioengineering* 96(1):18-26.
16. Yeh E, Garneau S, & Walsh CT (2005) Robust in vitro activity of RebF and RebH, a two-component reductase/halogenase, generating 7-chlorotryptophan during rebeccamycin biosynthesis. *Proceedings of the National Academy of Science USA* 102(11):3960-3965.